Alteration of cameroonian clays under acid treatment. Comparison with industrial adsorbents

ARTICLE *in* APPLIED CLAY SCIENCE · APRIL 2011

Impact Factor: 2.47 · DOI: 10.1016/j.clay.2011.02.009

Applied Clay Science 52 (2011) 122–132

Contents lists available at ScienceDirect

Applied Clay Science

journal homepage: www.elsevier.com/locate/clay

Research Paper

Alteration of cameroonian clays under acid treatment. Comparison with industrial adsorbents

J.P. Nguetnkam [a,c,*], R. Kamga [b], F. Villiéras [c], G.E. Ekodeck [d], A. Razafitianamaharavo [c], J. Yvon [c]

[a] Département des Sciences de la Terre, Faculté des Sciences, Université de Ngaoundéré, BP 454 Ngaoundéré, Cameroun
[b] Département de chimie Appliquée, Ecole Nationale Supérieure des Sciences agro-industrielles, Université de Ngaoundéré, BP 455 Ngaoundéré, Cameroun
[c] Laboratoire Environnement et Minéralurgie, LEM-ENSG, Nancy université-CNRS, 15 avenue du Charmois, BP40, 545001 Vandoeuvre-lès-Nancy, France
[d] Département des Sciences de la Terre, Faculté des Sciences, Université de Yaoundé I, BP 812 Yaoundé, Cameroun

ARTICLE INFO

Article history:
Received 8 September 2010
Received in revised form 3 February 2011
Accepted 9 February 2011
Available online 19 February 2011

Keywords:
Acid activation
Smectites
Kaolinite
Industrial adsorbents
Cameroon

ABSTRACT

In view to evaluate an alternative local cheaper source for vegetable oil refiners, three cameroonian clays containing swelling (smectites) and non-swelling (kaolinite) clay minerals were treated with sulphuric acid solutions at concentrations of 1, 2, 4 and 8 N at 80 °C for 2 h. Their alteration and resulting products were characterized by XRD, FT-IR-spectroscopy, chemical analyses, along with TEM-EDS, nitrogen adsorption isotherms at 77 K, and compared with industrial bleaching earths. Acid treatment of Cameroonian clays leads to the classically observed cristallochemical and textural modifications. The plot of TEM-EDS data in Al_2O_3/SiO_2 and Fe_2O_3/Al_2O_3 diagrams indicate that upon acid treatment, clay particles principally move towards the SiO_2 pole, consistent with the formation of an amorphous compound mainly siliceous as the result of acid activation. Concomitantly, a progressive decrease in cation exchange capacity (CEC) was observed with increasing sulphuric acid concentrations while both specific surface area and mesoporosity of the studied materials increase. Elemental analyses, X-ray and spectroscopy data reveal that acid activation affects both the octahedral and the tetrahedral sheets. The analysis of their reactivity shows that clays with high amounts of smectite are more sensitive to acid leaching than those with relative large kaolinite contents. Further, upon acid treatment, most trace and rare earth elements are leached, and the amount of toxic elements (e.g. Cd, Pb, Ni, Cu, As, Zn) in the by-products is low (<50 mg/kg). Mineralogy, chemical analyses and textural properties of the activated products match the specifications of industrial adsorbents. Therefore, activated Cameroonian clays are expected to perform well in respect with decolorization of vegetable oils.

1. Introduction

Clay minerals are essentially materials of very fine particle size, generally less than 2 μm; they form an important group of the phyllosilicate family of minerals, which are distinguished by layered structures composed of polymeric sheets of SiO_4 tetrahedra linked to sheets of $(Al, Mg, Fe)(O, OH)_6$ octahedra. Clay minerals are characterized by their cation exchange capacity, swellability and surface area. The best known and the most commonly used industrial clay minerals are kaolinite and different minerals of the smectite group.

Acid activation of clays is a treatment frequently used to enhance clay properties, mainly their sorptive properties (Brückman et al., 1976; Christidis et al, 1997; Espantaleon et al., 2003; Falaras et al., 1999, 2000; Nguetnkam, 2004; Rhodes and Brown, 1992; Srasra et al., 1989; Stoch et al., 1979a,b; Su rez Barrios et al., 1995; Vicente Rodriguez et al., 1996). In fact, like inorganic acid, clay surfaces can be highly acidic; and the acidity of the clay is crucial for its bleaching performance. Bronsted acid are sites generated by the exchange of interlamellar cations with protons and Lewis acid correspond to Mg^{2+} and Al^{3+} present at the edges of octahedral sheets (Kumar et al., 1995). Molinard et al. (1994) pointed out that in the acid-activated montmorillonite, the surface hydroxyl groups on the broken alumina sheets create a kind of adsorption sites in a similar way as in the case of the alumina pillars of an alumina pillared clay in acidic conditions. The protonated $AlOH^{+}_2$ structure can serve as an effective binding site permitting the attachment of pigments and other colouring matters contained in the vegetable oils. Furthermore, the catalytic activity of activated clay can be attributed to both the hydrolic and hydrophobic character of the clay surface. The protaned clay framework, highly hydrophilic in character, attracts the polar pigments. On the contrary, extensive leaching of cations from the octahedral sheet transforms the material to essential hydrophobic silica which serves to adsorb the non-polar colouring matters contained in the vegetable oils (Falaras et al., 1999). Acid activated clays are widely applied in the purification, decolorization and stabilization of vegetable oils, forest and water conservation, the mineral oil industry, environmental protection, the paper industry as well for cleaning and as detergents (Christidis et al., 1997; Clarke, 1985; O'Driscoll, 1988).

* Corresponding author at: Département des Sciences de la Terre, Faculté des Sciences, Université de Ngaoundéré, BP 454 Ngaoundéré, Cameroun. Tel.: +237 77386081.
E-mail address: jpnguet@yahoo.fr (J.P. Nguetnkam).

0169-1317/$ – see front matter © 2011 Elsevier B.V. All rights reserved.
doi:10.1016/j.clay.2011.02.009

Solutions of various concentrations of inorganic mineral acids are typically used for the acid treatment of clays. During the acid attack, the central atoms from octahedra as well as tetrahedral Al are removed from the clay structure (Christidis et al., 1997). The fastest part of such a process is the removal of the exchangeable cations and their substitution by protons. The extent of the dissolution reaction depends on the clay type, the acid strength and reaction conditions, such as the acid/clay ratio, time and temperature used (Rhodes and Brown, 1992; Srasra et al., 1989; Zaki et al., 1986). The final reaction product of acid treated clays is amorphous, porous, protonated and hydrated silica with a three-dimensional cross-linked structure (Breen et al., 1995, 1997; Christidis et al., 1997; Falaras et al., 1999; Tkac et al., 1994; Vicente Rodriguez et al., 1996). The most important physical changes in activated clays are the increase of their specific surface area and the average pore volume (Morgan et al., 1985; Rhodes and Brown, 1992; Srasra et al., 1989). A combination of several methods is needed to monitor morphological, textural and chemical changes during acid activation.

In Cameroon, vegetable oils refining is an important economical activity. Refiners cover their needs for acid activated clay entirely by imports, but their cost, most of it for transport, is relatively high. Nevertheless, Cameroon is potentially provided as far as clayey materials are concerned. In view to evaluate alternative local cheaper sources, prior to bleaching experiments, Cameroonian clays have been treated with sulphuric acid. In a previous study, Nguetnkam et al. (2005) assessed the surface areas of silica and clay in acid-leached clay materials by using concepts of adsorption on heterogeneous surfaces. They demonstrate that increasing acid concentration results in an increase in the surface area of silica, whereas the surface area of the protonated clay minerals remains roughly constant.

The present contribution is focussed on the morphological, textural and chemical evolution of Cameroonian clay mineral particles during acid treatment. The amount of toxic elements is also determined. The observed chemical and physical transformations are compared with results from literature on acid activation of smectites and kaolinites. Comparative information on industrial adsorbents was also included to discuss on the potential use of the modified clays for vegetable oil refining.

2. Materials and methods

The three clay materials used in the present study were sampled from pellic vertisols located in the Far North of Cameroon in the areas of Kaélé (10°08′N and 14°28′E), Maga (10°51′ and 14°57′E) and Kousseri (12°05′ and 14°90′). Clay fractions (<2 μm) were separated by sedimentation, decantation and subsequent drying at 105 °C.

Acid activations were carried out using analytical grade H_2SO_4, with concentrations varying between 1 N and 8 N at the temperature of 80 °C, a solid/liquid ratio of 1:5 (mass/volume). Four different sulphuric acid concentrations were used; 1, 2, 4 and 8 N. The slurry was stirred magnetically for 2 h. At the end of each run, and after cooling at room temperature, suspensions were filtered and the collected solid phases were washed several times with pure water (MiliQ ultrafiltration) until the filtrates were neutral. The obtained activated clays were then dried at 110 °C, gently ground in an agate mortar.

Activated clays of the area of Kaélé will be designated as Kaélé1N, Kaélé2N, Kaélé4N, and Kaélé8N, those of the area of Maga as Maga1N, Maga2N, Maga4N and Maga8N, and those of the area of Kousseri as Kous1N, Kous2N, Kous4N and Kous8N. The initial clays are referred as Kaélé0N, Maga0N and Kous0N.

For comparison, characteristics of three industrial acid treated adsorbents are given: Fulmont AA, Flor B80 and Enge. Fulmont AA is a product of Laporte Inorganic Co (Great Britain), Flor B80 was obtained from South Africa, and Enge from Engelhard Co (The Netherlands).

X-ray diffraction (XRD) was performed on oriented samples with a D8 Bruker diffractometer with Co Kα1 radiation (λ = 1.7902). Experimental conditions were, 35 kV, 45 mA, step scan 0.036° and step time 3.0 s. For further characterization of the swelling clay, the Greene-Kelly test was performed (Greene-Kelly, 1957; Hoffman and Klemen, 1950) in view to differentiate smectites with tetrahedral substitution (beidellite) to that with octahedral substitution (montmorillonite). To this end, the clay fraction was solvated with ethylene glycol.

Infrared spectra were recorded using an IFS 55 Bruker Fourier Transform IR spectrometer equipped with a MCT detector (6000–600 cm^{-1}) cooled at 77 K and in diffuse reflectance (Harrick attachment) mode. The amount of clay was 70 mg diluted in 370 mg of KBr. The spectra were recorded by accumulating 200 scans at 4.0 cm^{-1} resolution. IR spectra are shown in absorbance units.

Cation exchange capacity (CEC) was measured by using the chloride salt of cobalt hexamine $[Co(NH_3)_6Cl_3]$ as an exchangeable probe. The amounts of cobalt hexamine exchanged from the solution were determined by UV spectroscopy at wave number 473 nm. The exchanged cations displaced by cobalt hexamine were analysed by atomic absorption spectrometry (Perkin-Elmer 1100B). The pH values of clay suspensions were estimated at equilibrium conditions with a standard LPH 330T electrode.

Chemical analyses were performed at the "Centre de Recherches Pétrographiques et Géochimiques" (CRPG, Nancy, France) by emission spectrometry using inductively coupled plasma source and atomic emission spectroscopy (ICP-AES) for major elements, and mass spectrometry (ICP-MS) for trace elements after fusion with $LiBO_2$ and dissolution in HNO_3. Relative analytical uncertainties are estimated at 1–2% for major elements (5% for P_2O_5). They reach 5% for most of the trace element concentrations except for Cu and Ni (10%). However, uncertainty is high (>10%) for any trace element displaying a low concentration (<0.1 ppm).

TEM observations were carried out on clay fractions, with a Philips CM20 microscope equipped with an EDS detector at the common microscopy service of Nancy University.

Nitrogen adsorption–desorption isotherms at 77 K were recorded on a step by step automatic home built set-up. Specific surfaces areas (SSA) were determined from adsorption data by applying the Brunauer–Emmet–Teller (BET) equation. Micropore volumes and non-microporous surface areas were obtained using the *t*-plot method proposed by de Boer et al. (1966). Pore size distributions were calculated on the desorption branch using the Barrett–Joyner–Halenda method assuming parallel pore shape (Barrett et al., 1951).

3. Results

In our previous publication (Nguetnkam et al., 2005), we used low-pressure argon adsorption to determine the surface areas of both the amorphous silica formed and the protonated clay minerals in clays samples from Kaele and Kousseri, after activation with sulphuric acid. Prior to that determination, characteristics of those two natural Cameroonian clays and their activated products were given. Therefore the present results will be mainly focussed on clays from Maga, and industrial adsorbents, although some data concerning Kaele and Kousseri could be reminded.

3.1. X-ray diffraction

From X-ray patterns of the three natural clays it can be seen, that mainly poorly structured smectites identified by their broad basal spacing, d_{001}, which range from 14.2 to 15.2 Å are present in the samples (Fig. 1). Smectite basal spacing (d_{001}) expands to 17.4–18.2 Å with ethylene glycol. In the Greene-Kelly test the basal peak splits into two bands at 17.8 Å (beidellite) and 9.6 Å (montmorillonite), which indicates that these smectites consist in a mixture of beidellite and montmorillonite. Kaolinite is identified in the natural cameroonian clay by its basal

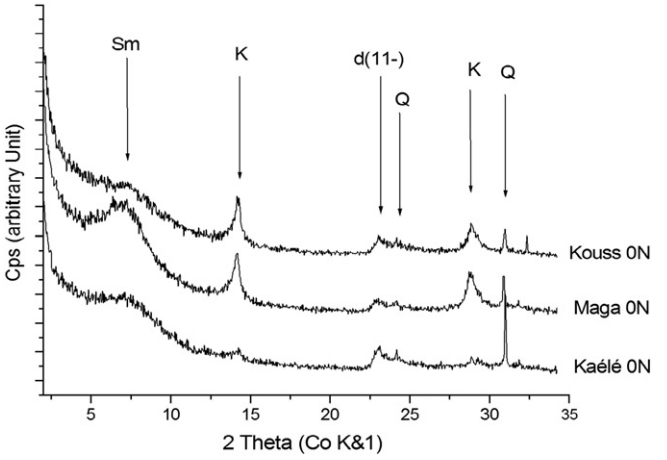

Fig. 1. X-ray diffraction patterns obtained on the <2 μm fraction of natural clay samples. The patterns are shown with an offset.

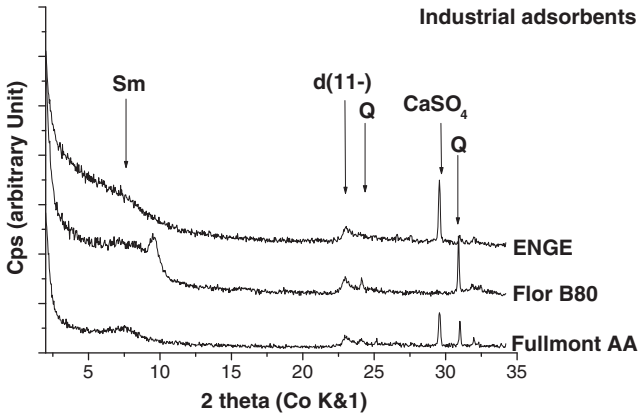

Fig. 3. X-ray diffraction of industrial adsorbents.

spacing at 7.2 and 3.6 Å, and constitutes the minor clay phase. Quartz is also present in minor amounts. Clays of Maga and Kousseri are richer in kaolinite (12% and 20%) than those of Kaele (9%), as deduced from the intensities of the peak at 7.2 Å, but they display lower quartz contents. Results of the semi-quantitative analysis show that sample Kaele is richer in smectites (85%) than those of Maga and kousseri (79% and 76%). The X-ray patterns of clays from Maga treated with 1, 2, 4 and 8 N H_2SO_4 solution, presented in Fig. 2, show that acid activation has caused structural changes in the treated clays, in agreement with the results obtained with Kaele and Kousseri samples. Activation has affected mainly the d_{001} basal spacing of smectites and kaolinite. In a first approximation, it can be observed that the crystallinity of samples decreased with increasing acid concentrations. The (d_{001}) basal reflections of smectites clearly decrease in intensity with treatment up to 2 N, and totally disappear after leaching with 4 N and 8 N H_2SO_4. A significant increase in the background noise which could be tentatively assigned to the formation of amorphous products is also observed. The decrease in the **(d_{001})** intensity can be related to a change in the lattice order along the c axis, denoting a growing delamellation of the clay particules as acid concentration increases.

The d_{001} and d_{002} reflections of kaolinite also decrease and broaden with acid concentration suggesting an increased crystalline disorder, but remain present even on the 8 N sample. The secant planes (11-) remain present for the whole range of concentration, which reveals that clay layers are not fully dissolved; but its peaks broaden with acid strength indicating also an increasing crystalline disorder.

As a conclusion, XRD patterns of activated clays indicate that acid leaching affects the d_{001} reflections of clay minerals and results in intense structural modifications. No additional crystalline phase is observed in reaction products showing that crystalline disorder is accompanied by the possible formation of an amorphous phase.

Commercial available industrial adsorbents display XRD patterns generally similar to those of activated cameroonian clays (Fig. 3). The presence of the typical secant planes (11-) indicates that they originate from clay materials. In addition to smectite and quartz, the samples Fulmont AA and Enge contain anhydrite. Kaolinite is not observed in these samples, but sample Flor B80 contains some illite.

3.2. Infrared spectroscopy

The study of the acid activated clays by FT-IR spectroscopy confirms that acid activation has caused structural changes in the treated clays. In fact, the IR data recorded herein indicate that both the octahedra and tetrahedra sheets were susceptible to acid attack, and also reveal the formation of amorphous silica. The spectra of untreated clay fractions from Maga and the samples treated with 1, 2, 4 and 8 N H_2SO_4 solution are shown in Fig. 4.

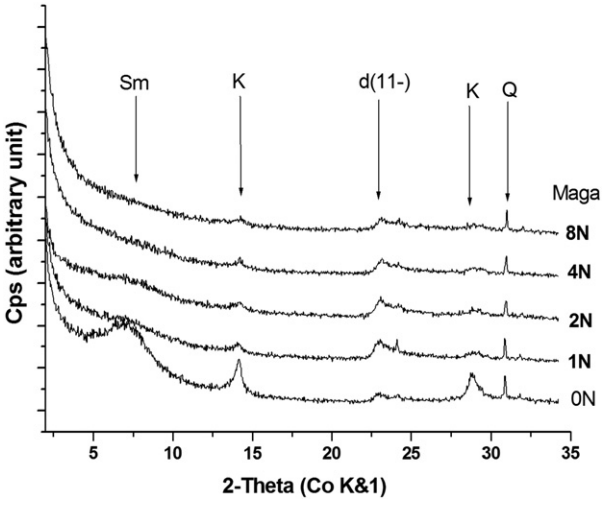

Fig. 2. X-ray diffraction patterns obtained on Maga activated samples. Sm: smectite, An: anhydrite, Q: quartz. d(11-): secant planes.

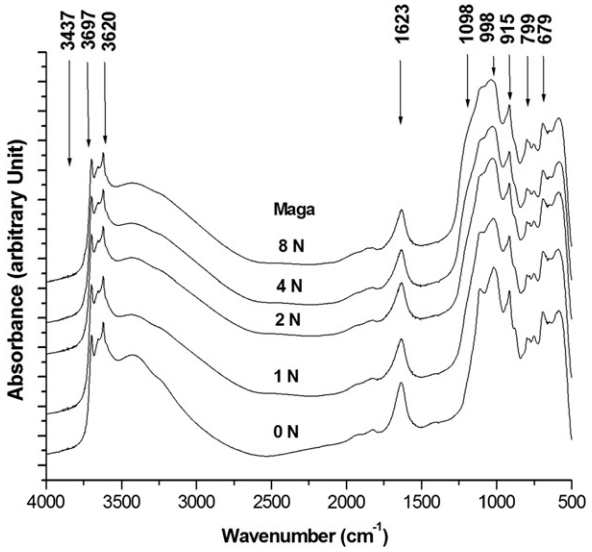

Fig. 4. Infrared spectra of natural and activated samples from Maga.

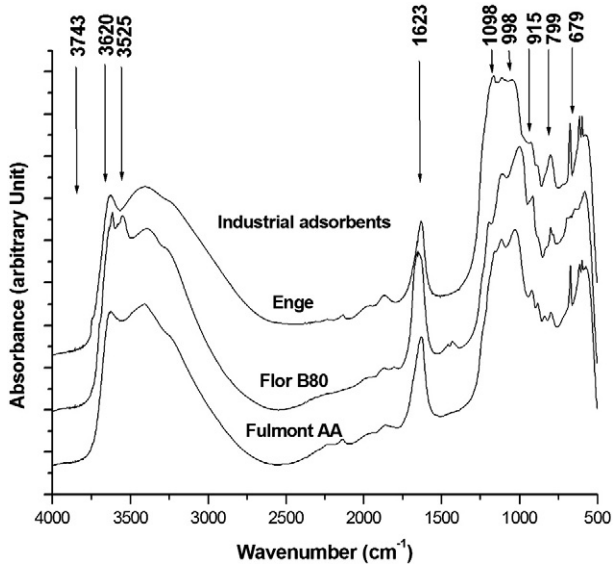

Fig. 5. Infrared spectra of industrial adsorbents.

As the treatment proceeds, the bands around 3400 cm^{-1} (OH-stretching vibration by adsorbed by water), becomes more diffuse and decrease with increasing the severity of the treatment. Similar behaviour was shown by the deformation band 1630 cm^{-1} (δOH vibration) suggesting the decrease in the amount of swelling clays. The bands at 915 cm^{-1} (deformation δOH of AlAl–OH) and at 880 cm^{-1} (deformation δOH of AlFe–OH) decrease and become very diffuse with the increase in acid concentration, suggesting a significant depopulation of the octahedra sheets. The bands at 1098 and 1020 cm^{-1} corresponding to δSi–O of the silicate network of clays, widen while the signal at 679 cm^{-1} (Si–O–Al) decreases with increasing acid concentration. These features show that the tetrahedral sheets are also affected during acid activation. The progressive widening of the 1098 and 1020 cm^{-1} bands together with the increase of the 799 cm^{-1} band indicate the formation of amorphous silica (Breen et al., 1995; Christidis et al, 1997; Falaras et al., 1999; Rhodes and Brown, 1992; Su rez Barrios et al., 1995; Vicente Rodriguez et al., 1996).

Kaolinite OH stretching vibrations between 3697 and 3620 cm^{-1} are still well expressed, even at 8 N, suggesting that kaolinite is less sensitive to acid leaching than smectite. This observation correlates well with XRD patterns of activated samples, in which the 001 reflections of kaolinite remain present even at H_2SO_4 8 N.

As a conclusion, IR spectra of activated clays indicate that acid leaching affects both the octahedral and the tetrahedra sheets, and reveal the formation of amorphous silica.

Industrial adsorbent did not present any characteristic band of kaolinite, which therefore confirms the XRD results. Their spectra are globally similar to those of activated Cameroonian clays (Fig. 5).

3.3. Behaviour of major elements

Elemental analysis, performed by ICP-AES provided clear evidence of the changes in the clay composition following acid activation (Table 1). The exchangeable cations, notably Ca and Na are strongly removed after the soft 1 N acid attack. The structural cations (Al, Fe and Mg) behave differently, being gradually removed from the clay lattice with increasing acid strength, while silica content relatively increases. As observed by Corma et al. (1987) and Luce et al. (1972), Mg^{2+} is the most released octahedral cation, whereas octahedral Al and Fe seem to be relatively resistant to acid attack. The loss on ignition of the activated clay is in the same range to that of the untreated sample (Table 1).

The net reduction in the CaO and Na_2O content indicated that both the Ca^{2+} and Na^{+} exchange cations were replaced by hydrogen ions and Al/or polycations leached from octahedral sheet. The decrease in the octahedral sheet oxides (MgO, Fe_2O_3, Al_2O_3) along with the concomitant increase in Si content proved that the original structure was altered. But a significant proportion of the octahedral cations remained, following acid activation by 8 N H_2SO_4, suggesting that the layered structure of the clay was not completely destroyed. The progressive increase in the silica content correlate well with the increase of the 799 cm^{-1} band and the appearance of the 3743 cm^{-1} band. The weak rate of leaching presented by K_2O is most probably due to the presence of highly stable K-feldspars or of illite that is often mixed with clay minerals as indicated in the clay particles observed by TEM analysis.

Activated cameroonian clays present chemical composition nearly identical to those of industrial adsorbents, the difference in oxide percent is generally less than 5%. Nevertheless, sample Fulmont AA and Enge are relatively richer in CaO and MgO, and relatively poor in Fe_2O_3 and Al_2O_3 than activated cameroonian clays. The lower content in Al_2O_3 may be due to the fact that industrial adsorbents do no contain kaolinite. Meanwhile their larger content in CaO and their higher loss of ignition value can be correlated to the presence of

Table 1
Major elements of natural and activated clays of Cameroon (<2 μm) and industrial adsorbents, and Mass balance (R). LOI: Loss on ignition. <ld: lower than detection limit. N/A: not applicable. Data of Kaele and Kousseri are from Nguetnkam et al., 2005.

Ref Echantillon	SiO_2	Al_2O_3	Fe_2O_3	MnO	MgO	CaO	Na_2O	K_2O	TiO_2	P_2O_5	LOI	Total	*R*
	%	%	%	%	%	%	%	%	%	%	%	%	
KOUSS 0N	44.74	26.64	8.59	0.03	1.04	0.71	0.19	0.95	1.65	0.15	15.18	99.87	100
KOUSS 1N	47.7	26.63	7.25	<L.D.	0.55	<L.D.	0.1	0.78	1.72	0.13	15.04	99.9	96
KOUSS 2N	48.88	26.16	6.2	<L.D.	0.48	<L.D.	0.1	0.74	1.81	0.13	15.09	99.58	91
KOUSS 4N	51.16	25.36	5.15	<L.D.	0.44	<L.D.	0.07	0.73	1.87	0.11	14.94	99.83	88
KOUSS 8N	54.2	23.76	4.07	<L.D.	0.37	<L.D.	0.08	0.79	1.95	0.12	14.41	99.75	85
MAGA 0N	45.2	24.27	9.2	<L.D.	1.15	1.11	0.19	0.72	1.13	0.1	16.79	99.86	100
MAGA 1N	48.97	24.24	8.56	<L.D.	0.67	0.29	0.07	0.69	1.26	0.11	15.63	100.49	90
MAGA 2N	50.07	23.44	7.52	<L.D.	0.59	0.25	0.07	0.66	1.28	0.09	15.88	99.84	88
MAGA 4N	51.92	22.71	6.28	<L.D.	0.5	0.24	0.09	0.63	1.34	0.09	16.08	99.87	84
MAGA 8N	55.33	21.25	4.91	<L.D.	0.41	0.18	0.11	0.65	1.42	0.1	15.55	99.91	80
KAELE 0N	47.82	22.31	9.14	0.05	1.84	1.39	0.55	0.95	0.98	0.08	15.36	100.47	100
KAELE 1N	51.16	21.45	8.28	<L.D.	1.09	0.42	0.17	0.8	1.06	0.07	15.34	99.83	92
KAELE 2N	53.42	20.99	6.98	<L.D.	0.96	0.32	0.18	0.76	1.12	0.08	15.48	100.29	88
KAELE 4N	56.54	19.52	5.31	<L.D.	0.76	0.28	0.14	0.77	1.18	0.07	15.28	99.84	83
KAELE 8N	60.5	17.41	3.94	<L.D.	0.58	0.26	0.2	0.8	1.25	0.07	14.84	99.85	78
FULLMONTAA	54.15	11.01	4.72	<L.D.	2.16	5.78	0.28	0.63	0.62	0.09	20.05	99.49	N/A
FLOR B80	57.22	11.94	4.86	0.03	5.34	1.78	0.2	1.04	0.48	0.73	16.21	99.83	N/A
ENGE	64.06	8.23	2.43	<L.D.	1.05	3.95	0.35	0.65	0.67	0.06	18.53	99.98	N/A

anhydrite. Sample Flor is richer in Mg and this can be explained by the fact that it was probably exchange with magnesium carbonate.

3.4. Behaviour of trace and Rare Earth elements

To be assured that the activated product**s** do not contain high amounts of toxic elements, trace and rare elements were determined for natural and activated samples of Kaele which are the most promising cameroonian adsorbents, and their compositions were compared with those of industrial adsorbents (Table 2).

3.4.1. Large lithophile elements (LILE: Rb, Cs, Ba, Sr, Th, U)

With increase sulphuric acid concentration, their amount decreased, except Ba which displayed an opposite trend (Table 2). In general their amount in activated cameroonian clays is lower than that of industrial adsorbents.

3.4.2. Transition trace elements (TTE: V, Cr, Co, Cu, Ni)

Their amount decrease with the increase of the concentration of sulphuric acid. V, Cr and Co contents in activated cameroonian clays are lower than that of Flor B80 and higher than that of the two other industrial adsorbents. Meanwhile Ni and Cu contents are relatively higher than that of the industrial adsorbents, but still low (<50 mg/kg).

3.4.3. High field strength elements (HFSE: Y, Zr, Nb, Hf)

The concentration of all HFSE decreases during acid treatment. Compared to industrial adsorbents activated Cameroonian clays display a relatively low content of HFSE.

Table 2
Trace and rare earth elements of natural and activated clays of Kaele (<2 μm) and industrial adsorbents.

REE (mg/kg)	KAELE 0 N	KAELE 1 N	KAELE 2 N	KAELE 4 N	KAELE 8 N	FULLMONT AA	FLOR B80	ENGE
La	38.01	26.97	25.86	24.84	24.54	93.8	24.5	84.59
Ce	58.53	32.44	31.63	30.71	28.79	188.7	44.82	183.6
Pr	9.133	4.8	4.49	4.184	3.762	20.64	5.525	21.53
Nd	35.18	16.84	15.51	14.16	12.33	70.87	20.79	78.52
Sm	7.054	2.921	2.625	2.396	2.095	12.24	3.952	13.49
Eu	1.633	0.611	0.53	0.475	0.41	1.893	0.825	2.794
Gd	5.819	2.219	1.879	1.722	1.581	9.119	3.343	9.365
Tb	0.903	0.364	0.312	0.285	0.26	1.463	0.518	1.416
Dy	5.179	2.216	1.913	1.741	1.664	8.366	3.082	7.699
Ho	1.001	0.441	0.391	0.361	0.335	1.586	0.597	1.326
Er	2.813	1.34	1.18	1.066	1.046	4.442	1.69	3.531
Tm	0.428	0.214	0.194	0.174	0.17	0.676	0.252	0.496
Yb	2.903	1.533	1.389	1.261	1.24	4.598	1.683	3.205
Lu	0.445	0.238	0.215	0.198	0.193	0.694	0.255	0.452
Total REE	169.03	93.147	88.118	83.573	78.416	419.087	111.83	412.01
S LREE	149.54	84.582	80.645	76.765	71.927	388.143	100.41	384.52
S HREE	19.491	8.565	7.473	6.808	6.489	30.944	11.42	27.49
LREE/HREE	7.672	9.875	10.792	11.276	11.084	12.543	8.793	13.988
Trace elements								
LILE (mg/kg)								
Rb	86.71	88.07	78.64	73.46	69.02	17.68	69.74	12.31
Cs	3.239	3.555	3.557	3.481	2.983	0.514	4.347	0.277
Ba	474.2	524.3	537	569.9	618.6	1132	224	163.3
Sr	154	97.28	91.82	90.8	92.87	87.03	77.18	1600
Th	10.19	6.222	5.035	4.606	4.608	12.73	7.877	8.124
U	6.302	2.12	1.916	1.847	1.846	3.838	2.036	2.348
Total	734.64	721.54	717.96	744.09	789.92	1253.792	385.18	1786.3
HFSE (mg/kg)								
Y	29.56	12.73	11.24	10.03	9.637	44.54	19.83	36.89
Zr	115	128.2	128.6	123.3	130.3	786.9	101.2	572
Nb	17.94	20.32	20.75	22.46	23.81	155	9.061	151.9
Hf	3.332	3.684	3.706	3.629	3.583	17.97	2.827	13.24
Total	165.832	164.934	164.296	159.419	167.33	1004.41	132.918	774.03
TTE (mg/kg)								
V	120.7	97.67	68.58	56.14	52.06	23.12	122.5	8.895
Cr	109.3	129.7	116.8	111.8	99.84	10.76	121.3	<L.D.
Co	15.12	9.595	7.915	6.377	5.085	1.965	31.48	0.455
Cu	45.48	40.53	31.97	24.47	18.86	3.558	9.262	<L.D.
Ni	47.79	46.54	41.98	41.21	35.94	9.741	27.97	<L.D.
Total	338.39	324.03	267.24	239.99	211.78	49.144	312.51	
Others trace elements (mg/kg)								
As	2.199	2.887	2.15	1.946	1.79	29.74	1.656	1.947
Be	2.743	1.452	1.186	1.147	0.977	1.234	1.47	<L.D.
Bi	0.246	0.234	0.252	0.278	0.247	0.142	0.209	0.197
Cd	<L.D.	<L.D.	<L.D.	<L.D.	<L.D.	0.483	0.507	<L.D.
Ga	28.77	29.64	26.94	23.44	20.34	25.3	14.79	17.87
Ge	1.641	1.753	1.826	1.902	1.913	1.091	1.505	0.799
In	0.099	0.079	0.08	0.071	0.061	0.099	0.072	0.067
Mo	0.697	1.068	1.077	1.139	1.101	2.502	0.667	0.54
Pb	14.303	15.927	16.063	16.938	18.381	28.4666	12.824	15.238
Sb	0.235	0.277	0.275	0.313	0.314	0.484	0.337	0.388
Sn	2.719	3.002	3.153	3.511	4.123	5.096	1.74	5.268
Ta	1.48	1.678	1.696	1.81	1.964	10.44	0.775	11.27
W	1.309	1.954	1.876	1.98	2.105	1.832	0.998	0.332
Zn	72	63.89	52.81	46.09	38.34	68.67	79.33	35.67

3.4.4. Other trace elements

With increase of acid concentration, As, Ge, Mo, Pb, Sb, Sn, Ta and W contents increase, while that of Be and Zn decrease. The amount of Cd is under the detection limit. The concentrations of all these trace elements in general are close to that displayed by the industrial adsorbents (Table 2).

3.5. Rare earth elements (REE)

During acid treatment, a general decrease is observed for LREE and HREE with the increase of the concentration of sulphuric acid, and the values obtained are lower or close to that of industrial adsorbents. The natural clays are richer in LREE and poor in HREE. This characteristic is maintained after treatment by sulphuric acid, and is also observed in industrial adsorbents.

At all, acid treatment induces leaching of most trace and rare earth elements, and the amount of toxic elements (e.g. Cd, Pb, Ni, Cu, As, Zn) in the by-products is low (<50 ppm).

3.6. Equilibrium pH and CEC of activated samples

The pH and the CEC of the natural clays from Maga progressively decrease with the increase of the sulphuric acid concentration, similar to the trend observed with clays from Kaele and Kousseri (Nguetnkam et al., 2005). The pH at equilibrium conditions of activated samples are remarkably low compared to initial samples (Table 3), but range between that of the industrial adsorbents. Sample Enge is the most acid industrial adsorbent; this may be due to the fact that it is richest in silica (Table 1) and may have the lowest buffering capacity for protons. Also, the CEC values of the activated samples range between the values of industrial adsorbents (26–53 meq/100 g).

3.7. Change in chemical composition of clay particles upon acid treatment

TEM-EDS analyses obtained on natural and activated Kaélé, Maga and Kousseri clays allow following the chemical evolution of clay particles upon acid treatment. Chemical compositions (wt.% oxides) are presented in Table 4, and indicate a few amounts of illites in those samples, in addition to smectite and kaolinite. Their projection in Al_2O_3/SiO_2 diagram (Fig. 6a,b,c) shows that clays from Kaele have an homogeneous average composition of smectite, while in Kousseri, two types of clays can be distinguished: pseudo hexagonal to hexagonal particles with kaolinite composition and aggregates of flakes and large curved particles with smectite average composition

Table 3
CEC and equilibrium pH of natural and activated clays of Cameroon (<2 μm). Data of Kaele and Kousseri are from Nguetnkam et al., 2005.

Samples	CEC meq/100 g	Na^+ mg/l	K^+ mg/l	Ca^{++} mg/l	Mg^{++} mg/l	pH
Kaélé 0N	74	46.9	16.3	143.3	27.9	8.3
Kaélé 1N	47	5 .0	12.3	39.7	13.4	4.9
Kaélé 2N	43	4.9	10.7	27.6	12.2	4.7
Kaélé 4N	36	4.3	9.5	25.0	10.1	4.7
Kaélé 8N	29	3.4	9.4	17.7	8.2	4.8
Maga 0N	64	17.0	6.2	127.8	29.3	8.7
Maga 1N	43	3.6	8.3	35.1	9.0	4.4
Maga 2N	41	2.8	6.9	28.8	8.4	4.3
Maga 4N	35	3.6	6.1	25.1	7.2	4.3
Maga 8N	27	2.4	6.6	18.4	5.7	4.4
Kouss 0N	38	11.8	5.7	79.3	19.5	7.6
Kouss 1N	26	2.9	6.9	11.4	5.5	4.6
Kouss 2N	24	2.9	6.5	8.3	4.8	4.5
Kouss 4N	21	2.4	5.9	7.2	4.0	4.5
Kouss 8N	18	2.1	5.9	6.7	3.6	4.6
Fulmont AA	53.84	1.5	5.2	604.3	13.6	5.2
Flor B80	34.69	2.8	7.7	60.8	27.5	6.2
Enge	26.37	3.3	1.2	437.5	6.2	3.0

Table 4
Chemical compositions (weight % oxides) deduced from TEM-EDS local analyses. (a) Kaélé, (b): Maga and (c) Kousseri. 01, 02, 03, … 10 correspond to different particles in the same sample.

Echantillons	SiO_2	Al_2O_3	Fe_2O_3	CaO	MgO	Na_2O	K_2O	Total
(a) Kaele								
KAE0N01	56.22	30.01	6.70	1.03	4.31	0.83	0.89	100.00
KAE0N02	56.97	30.67	5.62	1.10	3.93	1.24	0.47	100.00
KAE0N03	57.61	32.05	5.47	1.17	2.79	0.48	0.43	100.00
KAE0N04	57.42	31.48	6.24	1.26	2.78	0.52	0.31	100.00
KAE0N05	57.64	28.67	7.06	1.38	4.11	0.83	0.30	100.00
KAE0N06	53.64	28.81	5.15	7.25	3.84	0.97	0.35	100.00
KAE0N07	56.48	29.02	7.01	1.11	5.52	0.54	0.32	100.00
KAE1N01	60.10	32.41	4.29	0.38	2.50	0.00	0.33	100.00
KAE1N02	59.26	31.71	5.01	0.51	3.22	0.00	0.29	100.00
KAE1N03	60.61	29.07	5.56	0.19	3.47	0.93	0.17	100.00
KAE1N04	61.28	29.69	5.24	0.19	2.71	0.73	0.16	100.00
KAE1N05	61.64	30.94	4.19	0.19	2.22	0.18	0.64	100.00
KAE1N06	59.82	32.16	3.98	0.32	2.70	0.31	0.70	100.00
KAE1N07	60.45	28.17	6.58	0.35	2.69	1.01	0.75	100.00
KAE1N08	58.46	28.17	8.57	0.18	2.97	1.03	0.61	100.00
KAE1N09	57.74	36.28	3.05	0.19	2.22	0.36	0.16	100.00
KAE1N10	67.49	22.11	1.38	0.00	1.81	0.81	6.40	100.00
KAE2N01	63.81	28.37	5.19	0.18	1.94	0.35	0.16	100.00
KAE2N02	66.48	25.99	4.83	0.18	1.88	0.34	0.30	100.00
KAE2N03	67.60	22.22	1.22	0.00	0.89	0.72	7.35	100.00
KAE2N04	63.15	29.30	4.62	0.18	1.94	0.35	0.47	100.00
KAE2N05	55.54	37.88	3.32	0.38	1.82	0.74	0.33	100.00
KAE2N06	50.97	45.91	0.56	0.18	1.52	0.70	0.16	100.00
KAE2N07	70.17	21.82	4.36	0.36	2.33	0.51	0.46	100.00
KAE2N08	61.37	28.45	5.83	0.35	2.88	0.83	0.30	100.00
KAE2N09	58.56	31.86	3.70	0.34	2.67	0.50	2.37	100.00
KAE4N01	52.32	44.52	1.21	0.20	1.18	0.57	0.00	100.00
KAE4N02	66.11	27.06	3.88	0.18	1.94	0.52	0.31	100.00
KAE4N03	63.63	27.68	4.97	0.36	2.36	0.69	0.31	100.00
KAE4N04	60.40	33.88	2.57	0.18	2.14	0.69	0.15	100.00
KAE4N05	52.98	23.80	8.24	13.27	1.40	0.16	0.14	100.00
KAE4N06	68.40	23.01	1.39	0.00	1.42	0.49	5.29	100.00
KAE4N07	70.84	22.75	3.85	0.18	1.71	0.52	0.15	100.00
KAE4N08	52.82	38.14	1.60	0.00	2.48	0.33	4.63	100.00
KAE4N09	52.83	34.63	3.19	0.17	3.72	0.83	4.63	100.00
KAE4N10	89.11	8.62	0.91	0.18	0.85	0.34	0.00	100.00
KAE4N11	94.10	4.02	0.54	0.18	0.83	0.34	0.00	100.00
KAE4N12	66.96	27.18	4.27	0.36	0.22	0.70	0.31	100.00
KAE8N01	52.12	44.85	1.04	0.00	1.21	0.78	0.00	100.00
KAE8N02	89.49	7.99	0.95	0.19	0.88	0.36	0.16	100.00
KAE8N03	88.67	7.89	1.41	0.17	1.23	0.50	0.15	100.00
KAE8N04	65.48	30.13	2.30	0.19	1.56	0.18	0.16	100.00
KAE8N05	71.53	22.69	2.89	0.18	1.90	0.51	0.30	100.00
KAE8N06	68.71	25.89	2.98	0.17	1.63	0.33	0.29	100.00
KAE8N07	69.32	24.82	2.53	0.18	2.32	0.68	0.15	100.00
KAE8N08	51.84	45.43	0.60	0.19	1.39	0.37	0.17	100.00
KAE8N09	64.72	29.09	2.93	0.17	2.01	0.65	0.44	100.00
KAE8N10	59.93	35.89	1.91	0.19	1.56	0.36	0.16	100.00
(b) Maga								
MAGA0N01	55.47	32.02	9.50	1.38	1.32	0.04	0.28	100.00
MAGA0N02	55.36	32.48	9.23	1.16	0.78	0.00	1.00	100.00
MAGA0N03	56.37	40.20	3.13	0.31	0.00	0.00	0.00	100.00
MAGA0N04	56.63	32.91	8.79	1.00	0.15	0.00	0.52	100.00
MAGA0N05	51.02	32.66	6.82	0.37	0.95	0.27	7.91	100.00
MAGA0N06	57.65	28.38	11.13	1.53	0.88	0.05	0.37	100.00
MAGA0N07	55.58	27.36	13.53	1.49	1.62	0.00	0.43	100.00
MAGA0N08	57.39	35.86	6.01	0.74	0.00	0.00	0.00	100.00
MAGA0N09	97.47	1.61	0.48	0.06	0.00	0.33	0.05	100.00
MAGA0N10	5.71	1.55	92.17	0.56	0.02	0.00	0.00	100.00
MAGA0N11	55.74	29.35	12.99	1.75	0.02	0.00	0.15	100.00
MAGA0N12	54.67	31.18	11.76	1.13	1.27	0.00	0.00	100.00
MAGA0N13	98.31	1.49	0.00	0.00	0.00	0.11	0.09	100.00
MAGA0N14	55.12	29.88	9.85	1.25	1.00	0.42	2.48	100.00
MAGA0N15	94.88	3.44	1.30	0.17	0.00	0.21	0.00	100.00
MAGA0N16	63.54	18.20	0.64	0.00	0.00	0.72	16.90	100.00
MAGA0N17	66.95	30.53	2.31	0.20	0.00	0.00	0.01	100.00
MAGA0N18	59.67	35.07	4.70	0.49	0.00	0.00	0.07	100.00
MAGA0N19	56.12	34.78	7.33	0.96	0.49	0.00	0.32	100.00
MAGA0N20	56.75	36.42	5.17	1.42	0.00	0.00	0.24	100.00
MAGA0N21	54.14	38.80	6.15	0.71	0.00	0.00	0.21	100.00
MAGA4N01	72.99	19.27	7.20	0.32	0.22	0.00	0.00	100.00

(continued on next page)

Table 4 (*continued*)

Echantillons	SiO_2	Al_2O_3	Fe_2O_3	CaO	MgO	Na_2O	K_2O	Total
MAGA 4N 02	61.93	29.58	7.58	0.08	0.60	0.17	0.07	100.00
MAGA 4N 03	57.93	36.82	3.72	0.05	0.00	0.00	1.48	100.00
MAGA 4N 04	63.28	27.74	8.35	0.11	0.38	0.00	0.15	100.00
MAGA 4N 05	63.43	26.98	8.39	0.17	0.74	0.01	0.27	100.00
MAGA 4N 06	71.18	21.34	6.96	0.21	0.17	0.00	0.16	100.00
MAGA 4N 07	61.34	28.66	9.12	0.27	0.54	0.00	0.07	100.00
MAGA 4N 08	66.31	24.06	8.20	0.42	0.53	0.19	0.29	100.00
MAGA 4N 09	96.25	2.69	0.94	0.00	0.00	0.11	0.00	100.00
MAGA 4N 10	56.26	41.79	1.95	0.00	0.00	0.00	0.00	100.00
MAGA 4N 11	93.41	4.86	1.61	0.09	0.00	0.00	0.03	100.00
MAGA 4N 12	61.75	27.95	8.77	0.32	0.67	0.05	0.49	100.00
MAGA 4N 13	60.31	35.38	3.72	0.28	0.07	0.00	0.24	100.00
MAGA 4N 14	57.90	40.45	1.07	0.05	0.00	0.00	0.53	100.00
MAGA 4N 15	64.29	28.96	6.04	0.13	0.53	0.00	0.06	100.00
MAGA 4N 16	60.26	29.74	9.27	0.56	0.00	0.00	0.18	100.00
MAGA 4N 17	63.74	26.35	8.87	0.22	0.44	0.00	0.39	100.00
MAGA 4N 18	64.34	25.91	8.75	0.23	0.50	0.00	0.28	100.00
MAGA 4N 19	65.08	25.31	8.11	0.31	0.52	0.31	0.37	100.00
MAGA 4N 20	62.81	28.33	7.74	0.43	0.19	0.17	0.34	100.00
MAGA 4N 21	57.51	37.45	4.45	0.07	0.03	0.00	0.48	100.00
MAGA 4N 22	63.99	26.14	9.00	0.33	0.36	0.00	0.18	100.00
MAGA 4N 23	64.37	18.76	1.11	0.00	0.00	0.49	15.27	100.00
MAGA 4N 24	60.03	34.25	5.29	0.16	0.10	0.00	0.17	100.00
MAGA 4N 25	91.42	5.98	2.21	0.30	0.00	0.00	0.09	100.00
MAGA 4N 26	59.48	33.73	4.97	0.15	0.31	0.00	1.35	100.00
MAGA 4N 27	63.29	26.92	8.73	0.31	0.31	0.00	0.44	100.00
MAGA 4N 28	61.06	28.55	9.47	0.22	0.50	0.00	0.21	100.00
MAGA 4N 29	66.89	29.04	3.30	0.14	0.47	0.00	0.17	100.00
MAGA8N01	62.37	31.77	5.49	0.16	0.00	0.00	0.21	100.00
MAGA8N02	65.07	26.89	7.23	0.20	0.45	0.00	0.17	100.00
MAGA8N03	64.50	27.11	7.35	0.25	0.31	0.00	0.48	100.00
MAGA8N04	54.34	42.39	3.24	0.03	0.00	0.00	0.00	100.00
MAGA8N05	67.01	25.45	7.10	0.27	0.00	0.00	0.18	100.00
MAGA8N06	54.62	44.37	0.80	0.05	0.00	0.00	0.17	100.00
MAGA8N07	70.16	18.36	0.76	0.00	0.00	0.05	10.67	100.00
MAGA8N08	60.26	34.75	4.84	0.15	0.00	0.00	0.00	100.00
MAGA8N09	60.46	35.13	3.52	0.18	0.17	0.00	0.54	100.00
MAGA8N10	58.36	40.44	0.80	0.40	0.00	0.00	0.00	100.00
MAGA8N11	72.12	21.17	5.39	0.27	0.05	0.00	1.00	100.00
MAGA8N12	66.51	24.79	8.22	0.14	0.01	0.00	0.34	100.00
MAGA8N13	64.52	29.64	5.60	0.03	0.12	0.00	0.10	100.00
MAGA8N14	94.69	4.35	0.96	0.00	0.00	0.00	0.00	100.00
MAGA8N15	61.99	31.01	6.61	0.12	0.00	0.00	0.26	100.00
MAGA8N16	73.71	19.57	5.83	0.00	0.42	0.00	0.46	100.00
MAGA8N17	79.13	14.95	4.97	0.32	0.00	0.00	0.62	100.00
MAGA8N18	50.37	34.90	1.53	0.00	0.67	0.00	12.53	100.00
MAGA8N19	49.40	16.98	32.99	0.24	0.00	0.00	0.39	100.00
MAGA8N20	97.40	2.05	0.48	0.07	0.00	0.00	0.00	100.00
MAGA8N21	60.99	30.13	8.35	0.25	0.00	0.00	0.28	100.00
MAGA8N22	70.33	22.67	6.94	0.07	0.00	0.00	0.00	100.00
MAGA8N23	62.81	32.11	4.79	0.20	0.00	0.00	0.09	100.00
MAGA8N24	54.89	40.93	4.18	0.00	0.00	0.00	0.00	100.00
MAGA8N25	53.80	38.21	7.48	0.00	0.50	0.00	0.00	100.00
MAGA8N26	51.59	36.21	1.89	0.00	0.36	0.00	9.97	100.00
MAGA8N27	61.81	26.14	9.29	2.45	0.10	0.00	0.21	100.00
MAGA8N28	56.71	39.60	3.56	0.11	0.00	0.00	0.01	100.00
MAGA8N29	36.21	31.92	3.27	0.11	0.10	0.09	28.30	100.00
MAGA8N30	90.32	7.50	1.94	0.14	0.00	0.07	0.03	100.00
MAGA8N31	68.14	18.92	1.08	0.00	0.00	0.00	11.86	100.00
MAGA8N32	53.59	41.65	4.70	0.05	0.00	0.00	0.01	100.00
MAGA8N33	60.73	31.75	6.26	0.08	0.00	0.00	1.18	100.00
MAGA8N34	71.01	20.81	7.46	0.41	0.00	0.00	0.31	100.00
(c) Kousseri								
KOUS0N01	53.67	40.41	3.29	0.38	1.58	0.18	0.49	100.00
KOUS0N02	55.47	33.96	6.20	0.71	3.19	0.00	0.46	100.00
KOUS0N03	53.02	43.42	2.10	0.00	1.46	0.00	0.00	100.00
KOUS0N04	56.43	33.75	5.89	0.82	2.55	0.00	0.57	100.00
KOUS0N05	51.77	43.57	2.54	0.19	1.59	0.00	0.33	100.00
KOUS0N06	55.19	38.28	3.93	0.55	1.74	0.00	0.32	100.00
KOUS0N07	54.91	38.11	4.29	0.38	1.82	0.00	0.49	100.00
KOUS0N08	56.32	35.29	1.84	0.90	3.01	0.00	2.64	100.00
KOUS1N01	55.15	39.53	3.44	0.00	1.89	0.00	0.00	100.00
KOUS1N02	58.68	34.82	4.46	0.00	2.03	0.00	0.00	100.00
KOUS 1N03	57.79	35.88	4.56	0.00	1.77	0.00	0.00	100.00
KOUS 1N04	56.05	39.20	2.85	0.00	1.90	0.00	0.00	100.00

Table 4 (*continued*)

Echantillons	SiO_2	Al_2O_3	Fe_2O_3	CaO	MgO	Na_2O	K_2O	Total
(c) Kousseri								
KOUS 1N05	55.73	38.73	3.94	0.00	1.61	0.00	0.00	100.00
KOUS 1N06	55.00	39.31	3.38	0.00	2.31	0.00	0.00	100.00
KOUS 1N07	54.44	42.17	1.47	0.00	1.92	0.00	0.00	100.00
KOUS 1N08	57.78	35.39	4.80	0.00	2.03	0.00	0.00	100.00
KOUS 1N09	53.54	40.38	2.38	0.00	1.85	0.00	1.84	100.00
KOUS 1N10	57.12	34.98	3.81	0.00	2.57	0.00	1.52	100.00
KOUS 1N11	53.50	39.77	1.74	0.00	1.57	0.00	3.42	100.00
KOUS 1N12	56.47	37.27	4.09	0.00	2.16	0.00	0.00	100.00
KOUS 1N13	59.54	34.37	4.44	0.00	1.65	0.00	0.00	100.00
KOUS 2N01	59.37	36.59	4.04	0.00	0.00	0.00	0.00	100.00
KOUS 2N02	58.19	34.04	4.12	0.00	2.29	0.00	1.36	100.00
KOUS 2N03	57.65	36.08	3.66	0.00	1.79	0.00	0.81	100.00
KOUS 2N04	55.61	39.07	2.45	0.00	1.76	0.00	1.11	100.00
KOUS 2N05	57.68	40.15	2.17	0.00	0.00	0.00	0.00	100.00
KOUS 2N06	57.59	35.11	4.21	0.00	2.45	0.00	0.64	100.00
KOUS 2N07	54.67	41.49	2.93	0.00	0.91	0.00	0.00	100.00
KOUS 2N08	56.75	40.53	2.72	0.00	0.00	0.00	0.00	100.00
KOUS 2N09	61.98	32.14	5.88	0.00	0.00	0.00	0.00	100.00
KOUS 2N10	58.40	33.60	4.58	0.00	2.35	0.00	1.08	100.00
KOUS 2N11	55.17	43.35	1.47	0.00	0.00	0.00	0.00	100.00
KOUS 2N12	52.57	39.86	0.57	0.00	1.76	0.00	5.25	100.00
KOUS 2N13	63.97	25.01	6.44	0.00	4.58	0.00	0.00	100.00
KOUS 2N14	61.38	31.95	2.15	0.00	3.86	0.00	0.66	100.00
KOUS 2N15	50.64	42.46	0.73	0.00	1.70	0.00	4.46	100.00
KOUS 2N16	55.20	41.91	2.89	0.00	0.00	0.00	0.00	100.00
KOUS 2N17	56.12	41.90	1.98	0.00	0.00	0.00	0.00	100.00
KOUS4N01	57.56	35.85	4.59	0.00	2.00	0.00	0.00	100.00
KOUS4N02	54.09	42.99	2.92	0.00	0.00	0.00	0.00	100.00
KOUS4N03	57.64	38.79	2.46	0.00	1.10	0.00	0.00	100.00
KOUS4N04	64.49	28.87	4.88	0.00	1.76	0.00	0.00	100.00
KOUS4N05	63.44	17.11	19.44	0.00	0.00	0.00	0.00	100.00
KOUS4N06	77.10	20.16	2.74	0.00	0.00	0.00	0.00	100.00
KOUS4N07	58.44	36.24	3.73	0.00	1.60	0.00	0.00	100.00
KOUS4N08	74.64	22.69	2.67	0.00	0.00	0.00	0.00	100.00
KOUS4N09	57.32	40.62	2.06	0.00	0.00	0.00	0.00	100.00
KOUS4N10	62.80	32.90	3.44	0.00	0.00	0.00	0.87	100.00
KOUS4N11	56.30	38.23	3.45	0.00	2.01	0.00	0.00	100.00
KOUS4N12	59.64	34.32	3.27	0.00	1.69	0.00	1.07	100.00
KOUS4N13	57.03	39.63	2.82	0.00	0.00	0.00	0.51	100.00
KOUS4N14	56.94	41.09	1.97	0.00	0.00	0.00	0.00	100.00
KOUS4N15	54.07	45.93	0.00	0.00	0.00	0.00	0.00	100.00
KOUS4N16	57.24	38.69	2.57	0.00	0.00	0.00	1.50	100.00
KOUS4N17	76.83	20.32	2.85	0.00	0.00	0.00	0.00	100.00
KOUS4N18	61.83	32.41	5.77	0.00	0.00	0.00	0.00	100.00
KOUS8N01	56.61	41.05	1.83	0.00	0.00	0.00	0.51	100.00
KOUS8N02	66.44	30.62	2.95	0.00	0.00	0.00	0.00	100.00
KOUS8N03	54.33	40.34	2.17	0.00	0.00	0.00	3.16	100.00
KOUS8N04	65.26	31.52	3.22	0.00	0.00	0.00	0.00	100.00
KOUS8N05	66.75	29.67	3.59	0.00	0.00	0.00	0.00	100.00
KOUS8N06	64.99	31.97	2.71	0.00	0.00	0.00	0.33	100.00
KOUS8N07	55.82	38.58	1.50	0.00	0.00	0.00	4.10	100.00
KOUS8N08	66.97	30.15	2.88	0.00	0.00	0.00	0.00	100.00
KOUS8N09	61.99	31.02	3.80	0.00	0.00	0.00	3.20	100.00
KOUS8N10	58.76	38.66	2.58	0.00	0.00	0.00	0.00	100.00
KOUS8N11	61.15	36.24	2.61	0.00	0.00	0.00	0.00	100.00
KOUS8N12	61.34	35.47	3.19	0.00	0.00	0.00	0.00	100.00
KOUS8N13	74.69	23.03	2.28	0.00	0.00	0.00	0.00	100.00
KOUS8N14	66.09	30.80	3.11	0.00	0.00	0.00	0.00	100.00

similar to those of Kaele. Projection in Fe_2O_3/Al_2O_3 diagram (Fig. 7a, b, c) indicates that kaolonite from Kousseri are richer in Fe (Fig. 6c). Upon acid treatment, clay particles move towards two poles in the Fe_2O_3/Al_2O_3 diagram:

- a low Fe and Al content pole. Progression towards this pole leads to the formation of silica with a low amount of Fe and Al;
- a pole rich Al content pole. Evolution towards this pole leads to the formation of kaolinite. In fact, clay particles consist in a mixture of smectite and kaolinite. Therefore, activation destroys preferentially smectites particles, kaolinite particles seem to be more resistant. This correlates to IR spectra of activated clays in which the OH stretching vibrations of kaolinite between 3697 and 3620 cm^{-1} appears well expressed after acid treatment.

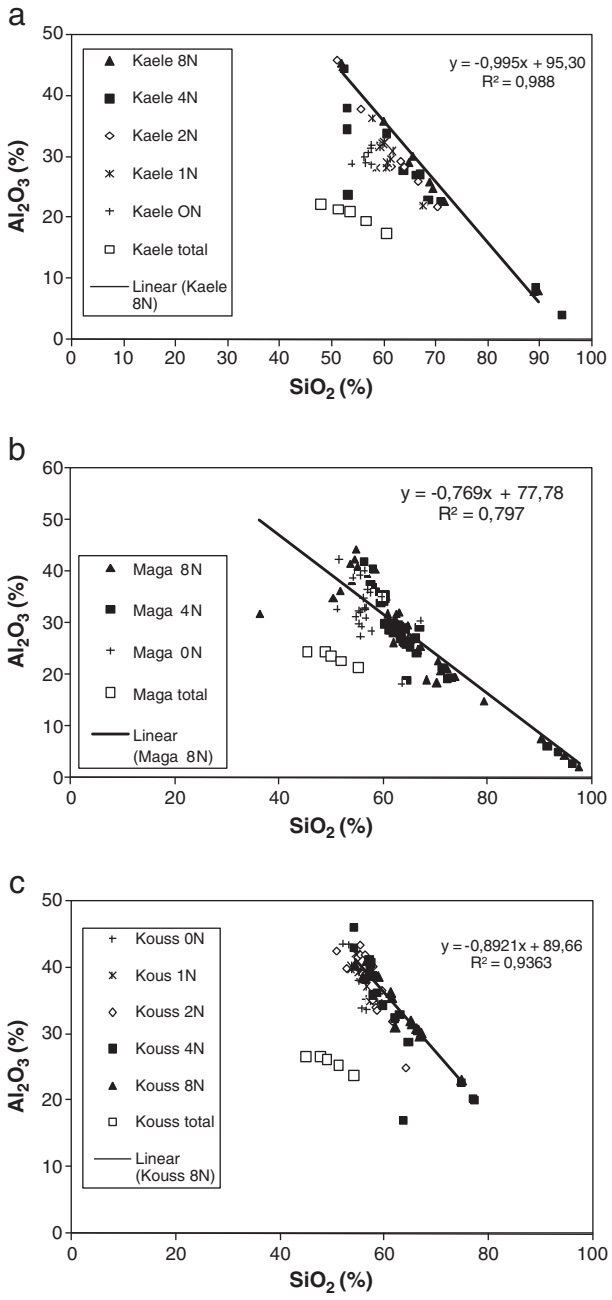

Fig. 6. Evolution of clay particles in Al_2O_3/SiO_2 diagram: (a) Kaele, (b) Maga and (c) Kousseri.

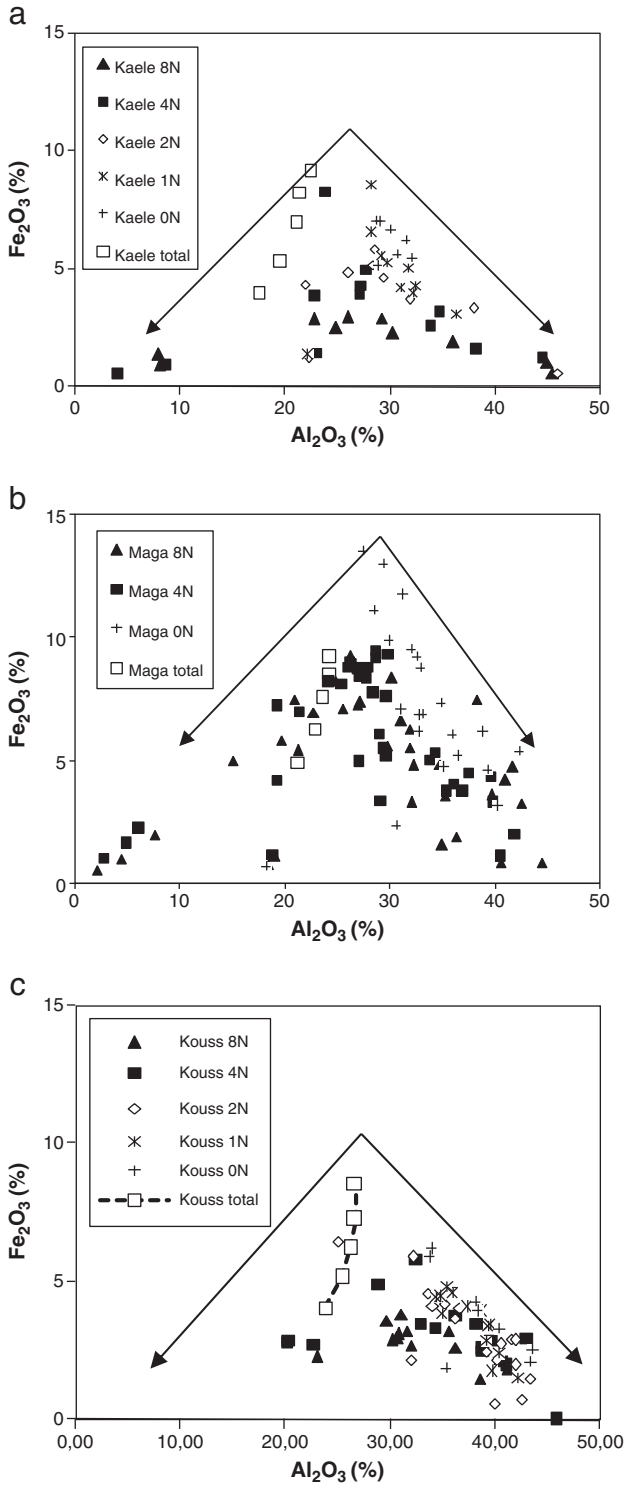

Fig. 7. Evolution of clay particles in Fe_2O_3/Al_2O_3 diagram: (a) Kaele, (b) Maga and (c) Kousseri.

The geochemical data obtained on the whole clay fraction by ICP-MS have also been plotted in the Al_2O_3–SiO_2 and Fe_2O_3–Al_2O_3 diagrams. It can be observed that after acid treatment, clay fractions display a trend similar to that of single clay particles, by moving towards the SiO_2 pole, although they are slightly switched (Figs. 6 and 7).

3.8. Textural properties

The natural cameroonian clays gave a specific surface area (SSA) which ranges between 81 and 110 m^2/g (Table 5). This value is within the typical surface area values for smectites (50–120 m^2/g) (Morgan et al., 1985; Van Olphen and Fripiat, 1979) and confirms that these clays consist mainly of very small particles as it is typically for smectites. For the three series, an important increase is visible from natural cameroonian clays (81–110 m^2/g) to the 8 N samples, which have a maximum in the SSA ranging between 160 and 212 m^2/g; this is about two times higher than that of the <2 μm of natural clays.

The microporosity derived from t-plot displays only marginal variations, independent of the concentration of the acid. It can then be concluded that acid leaching does not generate any micropores and that precipitated silica is not microporous. Evolution is different for mesoporosity that increases regularly with acid concentration suggesting that precipitated silica is mesoporous, as generally observed for amorphous silica gels (Su rez Barrios et al., 1995).

Table 5
Parameters resulting from the analysis of N_2 adsorption isotherms of activated clays. SSA: specific surface area. Data of Kaele and Kousseri are from Nguetnkam et al., 2005.

Sample	BET SSA (m^2 /g)	BET C constant	t-plot SSA (m^2 /g)	Microp. SSA (m^2 /g)	Microp. Volume (cm^3/g)	Mesop. Volume (cm^3/g)
Kaélé 0N	111	446	113	27	0.0009	0.145
Kaélé 1N	144	388	146	31	0.0011	0.183
Kaélé 2N	168	298	169	33	0.0012	0.192
Kaélé 4N	202	202	202	24	0.0009	0.231
Kaélé 8N	212	158	212	13	0.0005	0.279
Maga 0N	108	237	108	18	0.0007	0.148
Maga 1N	130	434	133	31	0.0011	0.184
Maga 2N	149	463	152	31	0.0011	0.188
Maga 4N	179	241	180	24	0.0009	0.211
Maga 8N	192	201	193	17	0.0006	0.255
Kouss 0N	81	208	81	12	0.0004	0.184
Kouss 1N	114	278	115	22	0.0008	0.223
Kouss 2N	126	287	127	22	0.0008	0.221
Kouss 4N	149	243	149	23	0.0008	0.243
Kouss 8N	161	174	160	15	0.0005	0.294
Fulmont AA	141	408	148	18	0.0007	0.250
Flor B80	154	154	153	12	0.0004	0.349
Enge	330	119	325	12	0.0004	0.441

Industrial adsorbents present similar SSA except for sample Enge (330 m^2/g). Microporosity was in the same range and mesopore volumes of Flor B80 and Enge samples are greater than those of all activated cameroonian samples.

4. Discussions

Acid treatment induces marked changes in the crystal structure of 1:1 and 2:1 layer silicates due to dissolution of structural ions and/or rearrangement of the structure. Generally, similar dissolution pathways are observed for various minerals under acid treatment involving structure destruction and formation of Si oxides (Jozefaciuk and Bowanko, 2002).

In the first part of this section, reactivity degree of three cameroonian clays to acid treatment will be discussed and the observed chemical and physical transformations will be compared with results from literature on acid activation of smectites and kaolinites. In the second part, the chemical and physical properties of obtained products will be compared with those of industrial adsorbents to discuss on the potential use of the modified clays for vegetable oil refining.

4.1. Reactivity of clays

The crystal and physical chemistry of the analysed samples determined by TEM-EDS and chemical analyses shows that acid activation results in a destabilization of the clay mineral followed by the precipitation of an amorphous compound mainly siliceous. In a concomitant way, both SSA and mesoporosity of the studied materials increase. It is possible to estimate the reactivity degree of clays upon acid treatment in term of mass by carrying out a mass balance. To realise this, it is possible to assume that TiO_2 is not sensitive to acid activation and that its quantity can be considered as invariant from one sample to another. On this basis, and after standardization to the mass of solid at 1100 °C (subtracting the ignition loss which includes adsorbed and structural water), the final weight (quantity of solid remaining / initial quantity) can be defined in the following way:

$$R(\%) = M^f / M^i = 100.TiO_2^i / TiO_2^f$$

where M^i and M^f correspond to the sample dry mass and, TiO_2^i and TiO_2^f to the initial and final contents (%) of TiO_2 before and after reaction, respectively. Obtained values (Table 1) show that reactivity is greater for sample Kaélé, which can be related to its larger content in smectite (85%) and its lower content in kaolinite (8%). Meanwhile, sample Kousseri, which is the one relatively rich in kaolinite (20%) displays the lower reactivity degree. Sample Maga sample (12% kaolinite) displays an intermediate reactivity degree. This observation suggests that kaolinite is most resistant to acid attack than smectite. This result is in conformity with the conclusions of Jozefaciuk and Bowanko (2002). In fact, studying the effect of acid and alkali treatments on surface areas and adsorption energies of selected minerals (bentonite, biotite, illite, kaolinite, vermiculite and zeolite), they observed that kaolinite was the most resistant mineral to acid attack; and this can be explained by the fact that kaolinite on acid treatment releases preferentially the octahedra Al ions from the clay structure and forms additional Al—OH and Si—OH bonds, without disturbing the mineral structure (Suraj et al., 1998). On the other hand, smectite is the most sensitive mineral to acid attack. Smectite is destroyed more rapidly than kaolinite because of its octahedral composition and its extralattice exchangeable cations (Breen et al., 1995; Christidis et al., 1997). Under acid treatment, smectites delaminate and partially dissolves. Activation proceeds with partial dissolution of smectite and is characterized by an initial replacement of the exchangeable cations in the interlayer space and external surface by H^+, followed by dissolution of the tetrahedral and octahedral sheets and subsequent release of the structural cations (Christidis et al., 1997). The final product of acid leaching of smectites is a hydrous amorphous silica phase (Komadel et al., 1990). These changes induce the decrease in CEC, and the increase of specific surface area and the average pore volume (Falaras et al, 1999; Rhodes and Brown, 1992; Srasra et al., 1989).

In this study, acid activation of three cameroonian clays displays a progressive decrease in cation exchange capacity (CEC) with increasing sulphuric acid concentrations; this can be understood in terms of the depletion of the octahedral sheet. In fact, it is well established that leaching of the octahedral cations (Mg^{2+}, Fe^{2+}, Al^{3+}) results in a reduction of the negative charge and therefore of the CEC (Breen et al., 1995; Falaras et al., 1999).

Moreover, there is a great difference between CEC values of activated clays measured by using cobalthexamine as an exchangeable probe and CEC values deduced from the chemical analysis of exchangeable cations. This difference can be assigned to the presence of exchangeable H^+ and Al^{3+} ions as suggested by the low equilibrium pH values of the samples. Such results then confirm that upon acid activation, most interlayer cations are replaced by H^+ ions (Breen et al., 1995; Falaras et al., 1999; Grim, 1962; Thomas et al., 1950). The acidity of clays plays an important role on their sorptive properties (Falaras et al., 1999; Kumar et al., 1995); it arises from H^+ ions occupying exchange sites on the surface or by dissociation of the water hydrating the exchange metal cation (Falaras et al., 1999). BrØnsted acid sites are generated by the exchange of

interlamellar cations with protons and Lewis acid sites correspond to Mg^{2+} and Al^{3+} present at the edges of octahedra sheets (Kumar et al., 1995).

Elemental analyses performed provided clear evidence of the change in the clay composition following acid activation. The net reduction in the CaO and Na_2O content indicated that both the Ca^{2+} and Na^{+} exchange cations were replaced by hydrogen ions and/or polyvalent cations leached from the octahedra sheet. The decrease in the amount of central cations in the octahedra sheet (Al, Mg, Fe) along with the concomitant increase in Si content proved that the original structure of clays was altered. These changes are supported by XRD and FTIR observations.

According to X-ray patterns, acid activation affects mainly the (d_{001}) reflections of the clay minerals. The d_{001} basal reflections of smectites progressively decrease and completely disappear with increasing acid sulfuric concentration, whereas the d_{001} reflections of kaolinite decrease and broaden, but remain present even on the 8 N sample, suggesting that kaolinite is less sensitive to acid attack than smectites. Moreover, secant planes are still observed for 8 N, which reveals that the layers of the clay minerals are not fully dissolved. The peaks broaden with acid strength indicating an increased crystalline disorder and/or a decrease in particle sizes.

FT-IR spectra of activated clays also confirm the partial destruction of the clay structure and the generation of amorphous silica during acid leaching. The characteristic bands of octahedral sheet of the silicate (915 cm^{-1} and 880 cm^{-1}) decrease with acid leaching, suggesting a significant depletion of the number of octahedra sheets (Falaras et al., 1999; Vicente Rodriguez et al., 1996). The changes in silicates can also be observed in the bands corresponding to its tetrahedral sheet. The 1098 and 1020 cm^{-1} bands (δSi—O of the silicate network of clays) widens while the signal at 679 cm^{-1} (Si—O—Al) decreases with increasing acid concentration. The formation of amorphous silica is suggested by the progressive widening of the 1098 and 1020 cm^{-1} bands coupled to the appearance of a 3743 cm^{-1} band (elongation vibration νOH of free Si—OH groups) and the increase of the 799 cm^{-1} band (Breen et al., 1995; Christidis et al, 1997; Falaras et al., 1999; Rhodes and Brown, 1992; Su rez Barrios et al., 1995; Vicente Rodriguez et al., 1996).

From the textural point of view, and as well documented, acid activation involves the increase in the specific surface area of the samples (Morgan et al., 1985; Rhodes and Brown, 1992; Srasra et al., 1989). The modification of the surface area is associated with changes in the clay structure during activation, mainly the formation of amorphous Si. The increase of the surface area under acid treatment may be caused by production of fine dispersed Si oxides from destruction of mineral structures, removal of amorphous Al or silica components plugging surface pores or interlamellar spaces, formation of the surface cracks and voids (Jozefaciuk and Bowanko, 2002).

The microporosity derived from the *t*-plots displays only marginal variations, independent of the concentration in acid. Thus, acid leaching does not generate any micropores and the amorphous silica formed is not microporous. In contrast, mesoporosity increases with the acid concentration. The silica is mesoporous, as generally observed for amorphous silica gels (Su rez Barrios et al., 1995).

The overall results obtained indicate that acid treatment of three cameroonian clays resulted in the known cristallochemical and textural modifications of clays under acid leaching (Brückman et al., 1976; Christidis et al, 1997; Falaras et al., 1999, 2000; Rhodes and Brown, 1992; Srasra et al., 1989; Stoch et al., 1979a,b; Su rez Barrios et al., 1995; Vicente Rodriguez et al., 1996).

4.2. Comparison with industrial adsorbents

Clay fractions from three cameroonian clays present quite different mineralogical, chemical and textural properties in comparison to that of industrial adsorbents. Following acid treatment, the physico chemical, mineralogy and textural properties of the activated cameroonian clay fractions are significantly improved and become very close to that of industrial adsorbents.

XRD patterns and IR spectra of industrial adsorbents are generally similar to those of activated cameroonian clays, and both contain amorphous silica. Activated cameroonian clays present chemical composition nearly identical to those of industrial adsorbents, the difference in oxide percent is globally less than 5% (Table 1). The CEC and pH-values of activated cameroonian clays range between those of industrial adsorbents (Table 3). From the textural point of view, industrial adsorbents, except for sample Enge that has a higher value (330 m^2/g), present SSA similar to those of activated Cameroonian clay samples, comprised between 110 and 215 m^2/g (Table 5). Microporosity was in the same range and mesopores volume of sample Flor B80 and Enge samples are greater than those of all activated cameroonian samples.

It is known that bentonites are highly valued for their sorptive properties which stem from their high SSA and their tendency to adsorb molecules in their interlayer sites (Christidis and Kosiari, 2003). Moreover, the SSA and surface acidity of activated smectites control, with some exceptions, decolorization properties (Christidis et al., 1997; Falaras et al., 1999; Morgan et al., 1985). Therefore the fact that the mineralogy, chemical analysis and textural properties of the activated cameroonian clays match the specifications of industrial adsorbents suggest that these activated cameroonian clays might be expected to perform well in respect with decolorization of vegetable oils. This has been confirmed by preliminary decolorization tests on cotton, maize and palm oils (Nguetnkam, 2004).

5. Conclusion

Acid treatment of three cameroonian clays results in the classically cristallochemical and textural modifications: partial destruction of the original clay structure, replacement of the interlayer cations by H^{+}, removal of octahedra cations, dissolution of the tetrahedral sheets, with formation of an amorphous silica. Concomitantly, the CEC progressively decreases while the SSA and mesoporosity of the studied materials increase. But acid leaching of cameroonian clays does not generate any micropores. Smectites are more sensitive to acid leaching than kaolinite.

The overall results obtained show that mineralogy, chemical analysis and textural properties of the activated products match the specifications of industrial adsorbents. Therefore, activated cameroonian clays might be expected to perform well in respect with decolorization of vegetable oils.

Acknowledgments

J.P. NGUETNKAM is grateful to the “Institut de Recherche pour le Développement” (IRD) for the grant making his visits to the “Laboratoire Environnement et Minéralurgie” (LEM). The suggestions and comments by Prof Daniel Njopwouo and an anonymous reviewer are appreciated.

References

Barrett, E.P., Joyner, L.G., Halenda, P.P., 1951. The determination of pore volume and area distributions in porous substances. I. Computation from nitrogen isotherms. J. Am. Chem. Soc. 73, 373–380.
Breen, C., Madejova, J., Komadel, P., 1995. Characterization of moderately acid-treated, size-fractionated montmorillonites using IR and MASNMR spectroscopy and thermal analysis. J. Mater. Chem. 5, 469–474.
Breen, C., Zahoor, E.D., Madejova, J., Komadel, P., 1997. Characterization and catalytic activity of acid-treated, size-fractionated smectites. J. Phys. Chem. B 101, 5324–5331.
Brückman, K., Fijal, J., Klapyta, Z., Wiltowski, T., Zabinski, W., 1976. Influence of different activation methods on the catalytic properties of montmorillonite. Mineral. Pol. 7, 5–17.
Christidis, G.E., Kosiari, S., 2003. Decolorization of vegetable oils: a study of the mechanism of adsorption of carotene by an acid-activated bentonite from Cyprus. Clays Clay Miner. 51 (N°.3), 327–333.
Christidis, G.E., Scott, P.W., Duhnam, A.C., 1997. Acid activation and bleaching capacity of bentonites from the islands of Milos and Chios, Aegan. Appl. Clay Sci. 12, 329–347.
Clarke, G.M., 1985. Special clays. Ind. Miner. 216, 25–51.
Corma, A., Misfud, A., Sanz, E., 1987. Influence of the chemical and textural characteristics of palygorskite on the acid leaching of octahedra cations. Clay Miner. 28, 225–232.

De Boer, J.H., Lippens, B.C., Linsen, B.G., Brokhoff, J.C.P., Van Der Heuvel, A., Osinga, T.J., 1966. The t-cuve of multimolecular N2 adsorption. J. Colloid Interface Sci. 21, 405–414.
Espantaleon, A.G., Nieto, J.A., Fernandez, M., Marsal, A., 2003. Use of activated clays in the removal of dyes and surfactants from tannery waste waters. Appl. Clay Sci. 24 (1), 105–110.
Falaras, P., Kovanis, I., Lezou, F., Seiragakis, G., 1999. Cottonseed oil bleaching by acid-activated montmorillonite. Clay Miner. 34, 221–232.
Falaras, P., Lezou, F., Seiragakis, G., Petrakis, D., 2000. Bleaching properties of alumina-pillared acid-activated montmorillonite. Clays Clay Miner. 48 (5), 549–556.
Greene-Kelly, 1957. The montmorillonite minerals (smectites). In: Mackenzie (Ed.), Differential Thermal Investigation of Clays. Mineralogical Society, London, pp. 53–59.
Grim, R.E., 1962. Applied Clay Mineralogy. McGraw-Hill, New York. 422 pp.
Hoffman, U., Klemen, R., 1950. Verlust der austauschfähigkeit von lithiumioen and bentonit durch erhitzung. Zeitsch. Anorg. Chem. 262, 95–99.
Jozefaciuk, G., Bowanko, G., 2002. Effect of acid and alkali treatments on surface areas and adsorption energies of selected minerals. Clays Clay Miner. 50 (N°.6), 771–783.
Komadel, P., Schmidt, D., Madejova, J., Cicel, B., 1990. Alteration of smectites by treatments with acid and sodium carbonate solutions. Appl. Clay Sci. 5, 113–122.
Kumar, P., Jastra, R.V., Bhat, T.S.G., 1995. Evaluation of porosity and surface acidity in montmorillonite clay on acid activation. Ind. Eng. Chem. Res. 34, 1440–1448.
Luce, R.W., Barlett, R.W., Parks, G.A., 1972. Dissolution kinetics of magnesium silicates. Geochim. Cosmochim. Acta 36, 35–50.
Molinard, A., Peeters, K.K., Maes, N., Vansant, E.F., 1994. Restoring the cation exchange capacity of alumina pillared montmorillonite trough modification with ammonium. In: Vansant, E.F. (Ed.), Separation Technology, Proc. Third Int. Symp. On Separation Technology. Elsevier Science, Amsterdam.
Morgan, D.A., Shaw, D.B., Sidebottom, M.J., Soon, T.C., Taylor, R.S., 1985. The function of bleaching earths in the processing of palm, palm kernel and coconut oils. J. Am. Oil Chem. Soc. 62, 292–299.
Nguetnkam, J.P., 2004. Les argiles des vertisols et des sols fersiallitiques de l'extrême Nord Cameroun: Genèse, propriétés cristallochimiques et texturales, typologie et applications à la décoloration des huiles végétales. Thèse Doctorat d'Etat, Université de Yaoundé I, 216 pp.
Nguetnkam, J.P., Kamga, R., Villiéras, F., Ekodeck, G.E., Razafitianamaharavo, A., Yvon, J., 2005. Assessment of the surface areas of silica and clay in acid leached clay materials using concepts of adsorption on heterogeneous surfaces. J. Colloid Interface Sci. 298, 104–115.
O'Driscoll, M., 1988. Bentonite; overcapacity in need of markets. Ind. Miner. 250, 43–67.
Rhodes, C.N., Brown, D.R., 1992. Structural characterization and optimization of acid-treated montmorillonite and high-porosity silica supports for $ZnCl_2$ alkylation catalysts. J. Chem. Faraday Trans. 88 (15), 2269–2274.
Srasra, E., Bergaya, F., Van Damme, H., Arguib, N.K., 1989. Surface properties of an activated bentonite. Decoloration of grape-seed oil. Appl. Clay Sci. 4, 411–421.
Stoch, L., Bahranowski, K., Gatarz, Z., 1979a. Bleaching properties of non bentonitic clay materials and their modification. II. Bleaching ability of natural and activated Krakowiec clays from Machow. Mineral. Pol. 10, 21–38.
Stoch, L., Bahranowski, K., Eilmes, J., Fijal, J., 1979b. Bleaching properties of non bentonitic clay materials and their modification: III. Modification of bleaching properties of Krakowiec clays from machow with some organic compounds. Mineral. Pol. 10, 39–47.
Su rez Barrios, M., Robert, M., Elsass, F., Martin Pozas, J.M., 1995. Evidence of a precursor in the neoformation of palysgorskite. New data by analytical electron microscopy. Clay Miner. 29, 255–264.
Suraj, G., Iyer, C.S.P., Lalithambika, M., 1998. Adsorption of cadmium and copper by modified kaolinites. Appl. Clay Sci. 13, 293–306.
Thomas, C.L., Hickey, J., Stecker, G., 1950. Chemistry of clay cracking catalysts. Ind. Eng. Chem. 42, 866–871.
Tkac, I., Komadel, P., Muller, D., 1994. Acid-treated montmorillonites—a study by 29Si and 27Al MAS NMR. Clay Miner. 29, 11–19.
Van Olphen, H., Fripiat, J.J., 1979. Data Handbook for Clay Materials and Other Non-Metallic Minerals. Pergamon Press.
Vicente Rodriguez, M.A., Suarez, M., Lopez Gonzalez, J.D., Banares Munoz, M.A., 1996. Characterization, surface area and porosity analyses of the solid obtained by acid leaching of a saponite. Langmuir 12, 566–572.
Zaki, I., Abdel-Khalik, M., Habashi, G.M., 1986. Acid leaching and consequent pore structure and bleaching capacity modifications of Egyptian clays. Colloids Surf. 17, 241–249.